

Far-infrared absorption of water clusters by first-principles molecular dynamics

Mal-Soon Lee,^{1,2} F. Baletto,^{1,a)} D. G. Kanhere,² and S. Scandolo^{1,3,b)}

¹*The Abdus Salam International Centre for Theoretical Physics, I-34014 Trieste, Italy*

²*Centre for Modeling and Simulation, and Department of Physics, University of Pune, Pune 411 007, India*

³*INFN/CNR "Democritos" National Simulation Center, I-34014 Trieste, Italy*

(Received 10 March 2008; accepted 30 April 2008; published online 3 June 2008)

Based on first-principle molecular dynamic simulations, we calculate the far-infrared spectra of small water clusters $(\text{H}_2\text{O})_n$ ($n=2,4,6$) at frequencies below 1000 cm^{-1} and at 80 K and at atmospheric temperature ($T > 200\text{ K}$). We find that cluster size and temperature affect the spectra significantly. The effect of the cluster size is similar to the one reported for confined water. Temperature changes not only the shape of the spectra but also the total strength of the absorption, a consequence of the complete anharmonic nature of the classical dynamics at high temperature. In particular, we find that in the frequency region up to 320 cm^{-1} , the absorption strength per molecule of the water dimer at 220 K is significantly larger than that of bulk liquid water, while tetramer and hexamer show bulklike strengths. However, the absorption strength of the dimer throughout the far-infrared region is too small to explain the measured vapor absorption continuum, which must therefore be dominated by other mechanisms. © 2008 American Institute of Physics.

[DOI: 10.1063/1.2933248]

I. INTRODUCTION

The dynamics of nanoscale water aggregates has recently attracted considerable interest due to the noticeable differences observed with respect to the dynamics of bulk liquid water, and to the implications that such differences may have in our understanding of solvation in biological environments.¹⁻³ Local changes in the molecular environment induced by confinement, solvation, or presence of an interface are known to affect substantially, in particular, the translational and librational modes in the far-infrared (far-IR) frequency range up to a few hundreds cm^{-1} . Similar to confinement, the presence of *open* boundaries such the ones found at the water-air interface and in gas-phase water nanoclusters is expected to have important effects on the far-IR dynamics of water, but these changes have not been investigated in full detail yet. The far-IR dynamics and absorption spectra of water nanoclusters have also an important role in atmospheric physics. Long-lived water clusters composed of up to a few water molecules are known to exist in non-negligible amounts in water vapor and in the atmosphere.^{4,5} Their concentration decays exponentially with the aggregate size, but molar fractions up to 10^{-3} have been suggested for the water dimer at typical atmospheric conditions, based on quantum chemical calculations.^{6,7} The relevance of small water clusters in our understanding of atmospheric phenomena is not fully understood, but it has recently been pointed out⁴⁻¹⁴ that they have an important role in the chemistry and in the radiation budget of the atmosphere, in particular, in the far-IR portion of the spectrum relevant for the greenhouse effect.^{4,15} The blackbody radiation emitted by Earth's surface

is peaked at $10\text{ }\mu\text{m}$ (1000 cm^{-1}) and has a large overlap with the far-IR absorption spectrum of water vapor. Current parametrization of the water vapor far-IR continuum reproduces the outgoing radiation spectrum accurately.¹⁵ However, the microscopic origin of the far-IR absorption of water vapor is still debated. Far-IR vapor continuum absorption is known to scale with the square of the water partial pressure, so models for its origin are either based on the collisionally broadened far-wing line shapes of the water monomer,^{16,17} or on the absorption of dimers.^{4,18,19} Accurate theoretical models of the far-wing line shape exist²⁰ and yield absolute absorption strengths in reasonable agreement with those reported for the vapor continuum.²¹ However, it has been claimed that the observed temperature dependence of the vapor absorption favors the dimer hypothesis,⁸⁻¹¹ although more recent theoretical studies show that the far-wing theory is capable of describing also the temperature dependence accurately.²² The measured vapor continuum is a monotonically decreasing function of frequency in the range between 300 and 1000 cm^{-1} .²¹ This behavior is qualitatively different from that of ice and bulk water,^{23,24} whose far-IR spectrum consists of one or two distinct peaks (see Fig. 1) and is far from monotonic in that frequency range. If the dimer hypotheses for the vapor continuum were proven correct, then this would point to a qualitative difference between the absorption of small freestanding water aggregates and that of bulk systems, similarly to what was reported for confined water aggregates.²

Theoretical approaches to model the far-IR absorption of water clusters have been so far based either on empirical potentials^{13,25} or on a potential fitted to far-IR data²⁶ or on more accurate quantum chemical calculations but only at zero temperature.²⁷ Calculations with empirical

^{a)}Present address: Physics Department, King's College London, UK.

^{b)}Electronic mail: scandolo@ictp.it.

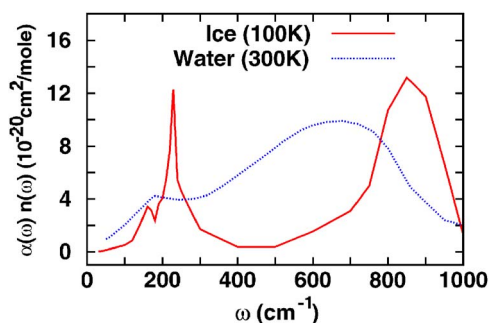


FIG. 1. (Color online) Experimental far-IR absorption spectra of ice and liquid water. Data are taken from Bertie *et al.* for ice (Ref. 23) and Robertson *et al.* for liquid water (Ref. 24).

potentials^{13,25} have yielded spectra characterized by the presence of several peaks and a clear nonmonotonic behavior. In Ref. 13, for example, the dimer spectrum shows a two-peak shape similar to that observed in bulk ice (see Fig. 1), but qualitatively different from the monotonic behavior of the measured vapor continuum. Results obtained with empirical potentials should be considered with caution, as empirical potentials have been shown to yield an incomplete description of the far-IR spectrum in the case of liquid water.²⁸ Quantum-mechanical perturbative approaches have been used to describe the near-IR OH-stretching modes of the dimer⁵ (however, some criticism has been raised also in this case, regarding line broadening²⁹). Accurate, all-atom potentials are being developed, particularly for the dimer.^{30–33} The calculation of the finite-temperature dimer far-IR absorption using one of these potentials fitted to far-IR transitions³⁰ has been recently reported.²⁶ However, the far-IR intermolecular classical dynamics of small water clusters is, at temperatures in the range of 200–300 K of interest for the atmosphere, comparable to that of a “melted” system,^{25,34} and it is sampling regions of the phase space which may be far from those sampled in far-IR experiments. Moreover, no attempt has been made so far to study with nonempirical methods water clusters larger than the dimer. Although slightly less accurate than quantum chemical methods, approaches based on the density-functional theory (DFT) are nonempirical and, when combined with molecular dynamics (MD), allow for the full dynamical treatment of finite-temperature effects, including classical anharmonicity, in much larger systems than the water dimer. First-principles DFT-based MD has been shown to reproduce the far-IR spectrum of bulk water systems (water and ice) with great accuracy^{28,35,36} and to lead to new insights into the intermolecular nature of the dynamical charge transfer responsible for the far-IR absorption of bulk water.²⁸ Here we calculate, by means of first-principles MD simulations, the absorption spectra of small water clusters at two different temperatures to study the effect of size and temperature on their spectra. We also estimate the contribution of the water dimer to the water vapor continuum, as measured by Burch,²¹ and find it to be small in the frequency range between 300 and 1000 cm^{-1} , in accordance with recent studies.²⁶

II. COMPUTATIONAL DETAILS

We performed first-principles, MD simulations of $(\text{H}_2\text{O})_n$ ($n=2,4,6$) at two different temperatures by using a pseudopotential, plane wave approach with energy cutoff of 80 Ry for the wave functions, in conjunction with a gradient corrected exchange-correlation functional [Becke–Lee–Yang–Parr (BLYP)], as implemented in the QUANTUM-ESPRESSO codes.³⁷ The choice of the BLYP functional was motivated by its excellent performance in describing the structural, energetic, and vibrational properties of small water clusters, as compared to higher level quantum chemical (MP2) calculations. Of particular importance to this study is the ability of BLYP to reproduce harmonic intermolecular vibrational frequencies ($\omega < 1000 \text{ cm}^{-1}$), which have been shown to deviate by at most 18 cm^{-1} from the MP2 values.³⁸

Atomic positions and electronic wave functions were evolved at finite temperature with the Car–Parrinello algorithm.³⁹ The electronic fictitious mass was set to a value of 250 a.u.,⁴⁰ and equations of motion were integrated with a time step of 5 a.u. Trajectories were initially equilibrated by means of a thermostat⁴¹ for about 1–2 ps, followed by microcanonical runs of up to at least 25 ps. Statistical averages were typically collected in the last 20 ps of the simulation.

Far-IR spectra were calculated from the Fourier transform of the time self-correlation of the total (electronic and nuclear) polarization. The absorption coefficient per molecule is defined as:^{35,42}

$$\alpha(\omega) = \frac{4\pi\omega \tanh(\beta\hbar\omega/2)}{3\hbar n(\omega)cN} \int_{-\infty}^{+\infty} dt e^{-i\omega t} \langle \mathbf{M}(t) \cdot \mathbf{M}(0) \rangle, \quad (1)$$

where N is the number of molecules in the cluster, T is the temperature, $\beta=1/(k_B T)$, $n(\omega)$ is the refractive index (in our case we take $n=1$ since we are considering an isolated system), c is the speed of light in vacuum, \mathbf{M} is the total dipole moment, and the angular brackets indicate a statistical average over initial times. The total dipole moment at each time step was evaluated using a Berry-phase approach.³⁵ Uncertainties due to the approximate nature of the quantum corrections in Eq.(1) were estimated by comparing the results to those obtained by replacing the \tanh term in Eq.(1) with its argument, as discussed in Ref. 43. Differences between the two formulations at $T > 200 \text{ K}$ amount to only about 20% of the total intensities. This is consistent with a study of quantum effects on the vibrational spectra of supercooled liquid water,⁴⁴ where similar corrections to the classical spectrum are found. Spectra at low T are instead subject to larger uncertainties both in terms of intensities (see Table I) and in terms of peak positions due to the fact that the dynamics used to generate the trajectories is classical. Inclusion of quantum anharmonicity can lead to a reduction of the harmonic frequencies by up to 40%.^{27,45} As a consequence, low-temperature spectra will only be used for qualitative comparisons.

TABLE I. Integral over frequency of the far-IR absorption strength per molecule (in units of 10⁻²⁰ cm). Integration up to 320 cm⁻¹ emphasizes the contribution of translational modes, while integration up to 1000 cm⁻¹ includes both translational and librational motion. Values in brackets refer to calculations using a different approximation for the quantum effects (see text, for details). Values for ice and liquid water are obtained from the experimental data of Bertie *et al.* (Ref. 23) and Robertson *et al.* (Ref. 24), respectively.

	T (K)	I ($\omega \leq 320$ cm ⁻¹)	I ($\omega \leq 1000$ cm ⁻¹)
Dimer	80	490 (740)	510 (830)
	220	1430 (1580)	1770 (2150)
Tetramer	270	720 (800)	1560 (2200)
Hexamer	220	630 (720)	1160 (1790)
Ice	100	780	3700
Water	300	890	5550

III. RESULTS AND DISCUSSIONS

A. Geometry

We started our simulations from the known ground state structures for the dimer and the tetramer (cyclic), as shown in Figs. 2(a) and 2(b), respectively.^{38,46} In the case of the hexamer several isomers are known to be almost degenerate in energy, so we optimized the parameters of four different initial structures with ring (also known as cyclic), book, cage, and prism geometry, respectively.⁴⁶ At our pseudopotential/BLYP level of theory, the ring structure [Fig. 2(c)] has the lowest energy among these four degenerate geometries. The obtained binding energies of the dimer, tetramer, and hexamer (ring), calculated after full relaxation of the atomic positions without inclusion of quantum effects, are 0.09, 0.27, and 0.30 eV/molecule, respectively, which compare favorably to MP2 calculations (0.095, 0.264, and 0.307 eV/molecule). Our calculated O–O distance for the dimer at low temperature is 2.95 Å, to be compared to the MP2 value of 2.91 Å.^{38,47} Moreover, differences between hexamer isomers are also found to be very small (the four

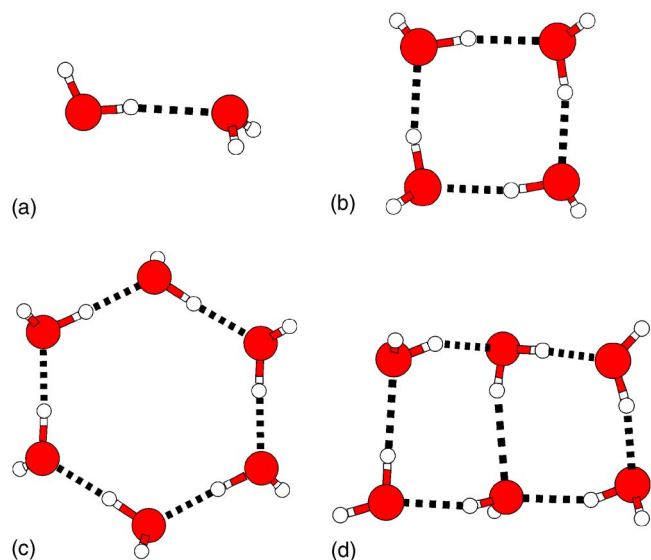


FIG. 2. (Color online) The ground state geometry of the dimer (a), tetramer (b), and hexamer (c). Also shown is a booklike structure (d) observed during the MD simulation of the hexamer at 220 K.

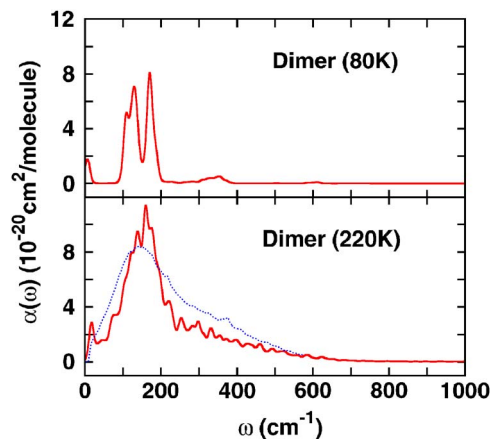


FIG. 3. (Color online) Calculated far-IR absorption spectra per molecule for the dimer. The spectrum obtained by Scribano and Leforestier (Ref. 26) (dotted line) is also shown, for the comparison.

isomers are within 0.02 eV), in fair agreement with the value of 0.03 eV from quantum chemical calculations.⁴⁷

Our MD simulations at two temperatures highlight differences between the classical quasiharmonic regime (80 K) and fully anharmonic regime relevant for the atmosphere (>200 K). At 80 K, molecules show only oscillations around their equilibrium positions for all the clusters studied. However, for the dimer at 220 K, we find large fluctuations of the intermolecular distance and angle and occasional exchanges of the hydrogen atoms pointing to the acceptor molecule, indicating a completely anharmonic classical dynamics. For the tetramer at 270 K, we observe a large fluctuation of the free (dangling) hydrogen atoms, but no hydrogen bond breaking or exchange, a likely consequence of the energetic stability of the ring isomer with respect to other (H₂O)₄ isomers.⁴⁸ For the hexamer we find that when the simulation is started with the cage structure, the system transforms upon heating into ring (via an intermediate state with booklike geometry). After equilibration the ring structure continues to exhibit large fluctuations which occasionally bring the structure into a booklike geometry, as shown in Fig. 2(d). A very similar behavior was observed when the simulation was started from the ring structure. The large thermal fluctuations observed for the hexamer are a consequence of the energetic quasidegeneracy of the book and ring isomers and of the simple transformation path between the two isomers. Our finding that temperature stabilizes more open structures is consistent with finite-temperature free energy calculations on the different isomers.⁴⁹

B. Far-IR spectrum

Calculated far-IR spectra at two representative temperatures of 80 and 220 K (270 K for tetramer) are reported in Figs. 3 and 4. Peak positions in the spectra calculated at 80 K are in fair agreement with harmonic IR frequencies and intensities calculated with quantum chemical methods.^{27,38} Due to the lack of quantum anharmonicity, our results may therefore overestimate the real frequencies by as much as 40%.^{27,45} The size dependence of the high temperature absorption spectra shows that the librational peaks (i.e., peaks

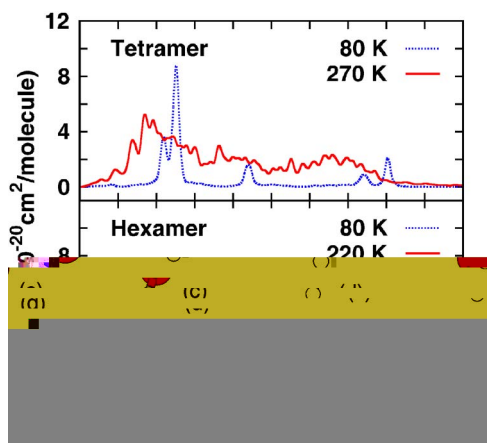


FIG. 4. (Color online) Calculated far-IR absorption spectra per molecule for the tetramer and the hexamer.

above 320 cm^{-1} in the low-temperature spectra) shift to higher frequency for increasing cluster size, which is similar to the trend reported for water confined in reverse micelles, as a function of the cavity size.² The intensity of the librational peaks is systematically smaller than in bulk systems and appears to be the largest in the case of the tetramer, an observation which might be related to the energetic stability, and thus geometrical rigidity, of the ring isomer in the case of the tetramer. The temperature dependence of the calculated IR intensities shows, for the dimer, a considerable broadening of the spectrum at 220 K. Contrary to previous empirical potential calculations,^{13,25} the dimer spectrum at 220 K is here found to decrease monotonically above 200 cm^{-1} , with a shape that resembles that of the observed vapor continuum. Strong temperature effects are found also in the case of the tetramer and hexamer. The librational peaks above 400 cm^{-1} start to merge and shift to lower frequencies for increasing temperature, although inclusion of quantum effects neglected in this work may reduce such shift. In the harmonic limit, broadening is generally accompanied by a decrease of the peaks heights, due to sum-rule constraints, at least so long as the molecular effective charges related to the intermolecular modes²⁸ can be considered temperature independent. In contrast, we find that the integral of the far-IR spectrum is strongly temperature dependent (see Table I), with an increase of more than three times between 80 and 220 K in the case of the dimer. This shows that not only the shape but also the total strength of the absorption is strongly temperature dependent, a likely consequence of the complete anharmonic nature of the dimer classical dynamics at 220 K. It is interesting to remark that a large increase in the total strength of the far-IR absorption is also seen in bulk water upon melting. The integrated spectrum of liquid water is, in fact, 1.5 times larger than that of ice. In absolute terms, we find that the absorption strength per molecule for the frequencies below 320 cm^{-1} is larger in the dimer at 220 K than in water at ambient conditions. A comparison of our results for the dimer at high temperature to the spectra obtained using an extrapolation to large rotational numbers of the transition elements calculated with an

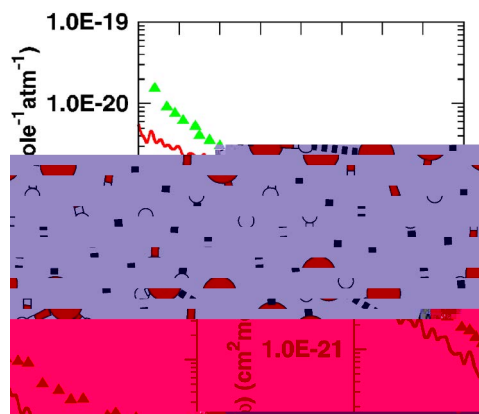


FIG. 5. (Color online) Calculated contribution due to water dimers to the water vapor at 296 K assuming a dimer partial pressure of 54×10^{-3} torr. The triangles show the experimental water vapor absorption coefficient measured by Burch *et al.* (Ref. 21).

all-atom potential,²⁶ shows that the two approaches agree in predicting a monotonic decrease of the absorption and their intensities above 200 cm^{-1} (Fig. 3).

C. Far-IR absorption of water dimer and water vapor continuum

Having obtained the far-IR absorption strength of water dimers, we now turn to the problem of determining whether absorption by dimers can explain the far-IR water vapor continuum. In order to compare our results to experimental data, the water partial pressure $P_{\text{H}_2\text{O}}$ and the partial pressure of dimers $P_{(\text{H}_2\text{O})_2}$ in water vapor must be specified. At standard conditions and 100% relative humidity, the water partial pressure $P_{\text{H}_2\text{O}}$ is 21 torr. $P_{(\text{H}_2\text{O})_2}$ is not known experimentally, but theoretical calculations suggest for $P_{(\text{H}_2\text{O})_2}$ values in the range of $(11\text{--}54) \times 10^{-3}$ torr.⁶ Absorption coefficient measurements for the water vapor are generally reported in the literature as absorption cross section per water molecule, normalized to the water partial pressure. The dimer contribution to the water vapor continuum $\alpha_{\text{dimer}}(\omega)$ is therefore given, in terms of $\alpha(\omega)$, by

$$\alpha_{\text{dimer}}(\omega) = 2\alpha(\omega) \frac{P_{(\text{H}_2\text{O})_2}}{P_{\text{H}_2\text{O}}^2},$$

where the factor of 2 accounts for the number of molecules in the dimer. The theoretical contribution from dimer absorption to the vapor continuum is compared to the experimental spectrum²¹ in Fig. 5, for the largest available value of $P_{(\text{H}_2\text{O})_2}$ (54×10^{-3} torr).⁶ The comparison shows that the calculated far-IR absorption due to dimers is significantly smaller than the observed water vapor continuum even for the largest value of the dimer concentration. Hence, it is highly likely that collisional broadening is the predominant mechanism responsible for the water vapor continuum. It has been remarked that the temperature dependence of the dimer contribution reproduces the observed temperature dependence observed for water vapor more closely than the collisional broadening.^{8–11} This conclusion was based on the assumption that the temperature dependence in the absorption cross

section is solely due to the dimer partial pressure, which is inconsistent with our calculated strong temperature dependence of the absorption coefficient per dimer. Interestingly, however, the shape of the theoretical dimer curve has a similar, monotonic behavior, indicating that the dimer absorption mechanism would explain the vapor continuum if the concentration of dimers in the vapor would reach values in the range of 0.1–0.2 torr, i.e., much larger than current theoretical estimates.

IV. CONCLUSIONS

The far-IR spectra of the water dimer, tetramer, and hexamer have been calculated by employing DFT-based MD simulations at two different temperatures. The librational peaks shift to higher frequency as the cluster size increases. The similarity between these trends and those reported for water confined within reverse micelles suggests a universal nature for the changes induced by confinement on the far-IR dynamics of water aggregates. Temperature effects are found to be important, both in the shape and in the intensity of the spectra. By comparing the calculated far-IR absorption of the dimer to the measured water vapor continuum, we conclude that even though the shape of the two spectra is similar, the intensity in the case of the water dimer is too small to account for the vapor continuum. The origin of the vapor continuum therefore cannot be explained solely by a dimer absorption mechanism. The agreement between our results for the dimer and those obtained recently by means of a potential fitted to far-IR data provides an important cross validation of the two methods. In particular, it suggests that DFT-based approaches are able to capture the relevant aspects of the water cluster dynamics with an accuracy comparable, at least for the scopes of the present work, to that of the best available all-atom potential calculation.

ACKNOWLEDGMENTS

We acknowledge partial support from INFN/CNR through “Iniziativa per il Calcolo Parallelo” and from MIUR through PRIN No. 2006020543. M.-S.L. acknowledge support from ICTP through the OEA/STEP program.

¹N. E. Levinger, *Science* **298**, 1722 (2002).

²D. E. Rosenfeld and C. A. Schmuttenmaer, *J. Phys. Chem. B* **110**, 14304 (2006); D. S. Venebles, K. Huang, and C. A. Schmuttenmaer, *ibid.* **105**, 9132 (2001).

³J. E. Boyd, A. Briskman, C. M. Sayes, D. Mittleman, and V. Colvin, *J. Phys. Chem. B* **106**, 6346 (2002).

⁴K. J. Bignell, *Q. J. R. Meteorol. Soc.* **96**, 390 (1970).

⁵K. Pfeilsticker, A. Lotter, C. Peters, and H. Bösch, *Science* **300**, 2078 (2003).

⁶N. Goldman, C. Leforestier, and R. J. Saykally, *J. Phys. Chem. A* **108**, 787 (2004).

⁷G. T. Evans and V. Vaida, *J. Chem. Phys.* **113**, 6652 (2000).

⁸A. A. Vigin, *J. Quant. Spectrosc. Radiat. Transf.* **64**, 24 (2000).

⁹G. L. Loper, M. A. O'Neill, and J. A. Gelbwachs, *Appl. Opt.* **22**, 3701

(1983).

¹⁰R. E. Roberts, J. E. A. Selby, and L. M. Biberman, *Appl. Opt.* **15**, 2085 (1976).

¹¹J. G. Cormier, J. T. Hodges, and J. R. Drummond, *J. Chem. Phys.* **122**, 114309 (2005).

¹²P. Chýlek and D. J. Geldart, *Geophys. Res. Lett.* **24**, 2015 (1997).

¹³H. C. W. Tso, D. J. W. Geldart, and P. Chýlek, *J. Chem. Phys.* **108**, 5319 (1998).

¹⁴S. H. Suck, A. E. Wetmore, T. S. Chen, and J. L. Kassner, Jr., *Appl. Opt.* **21**, 1610 (1982).

¹⁵P. F. Bernath, *Phys. Chem. Chem. Phys.* **4**, 1501 (2002).

¹⁶W. M. Elsasser, *Astrophys. J.* **87**, 497 (1938).

¹⁷P. W. Rosenkranz, *J. Chem. Phys.* **87**, 163 (1987).

¹⁸S. S. Penner and P. Varanasi, *J. Quant. Spectrosc. Radiat. Transf.* **7**, 687 (1967).

¹⁹P. Varanasi, S. Chou, and S. S. Penner, *J. Quant. Spectrosc. Radiat. Transf.* **8**, 1537 (1968).

²⁰Q. Ma and R. H. Tipping, *J. Chem. Phys.* **111**, 5909 (1999).

²¹D. E. Burch, *Proc. SPIE* **277**, 28 (1981).

²²Q. Ma, R. H. Tipping, and C. Leforestier, *J. Chem. Phys.* **128**, 124313 (2008).

²³J. E. Bertie, H. J. Labb, and E. Whalley, *J. Chem. Phys.* **50**, 4501 (1969).

²⁴C. W. Robertson, B. Curnutte, and D. Williams, *Mol. Phys.* **26**, 183 (1973).

²⁵W. B. Bosma, L. E. Fried, and S. Mukamel, *J. Chem. Phys.* **98**, 4413 (1993).

²⁶Y. Scribano and C. Leforestier, *J. Chem. Phys.* **126**, 234301 (2007).

²⁷M. E. Dunn, T. M. Evans, K. N. Kirschner, and G. C. Shields, *J. Phys. Chem. A* **110**, 303 (2006).

²⁸M. Sharma, R. Resta, and R. Car, *Phys. Rev. Lett.* **95**, 187401 (2005).

²⁹M. A. Suhm, *Science* **304**, 823 (2004).

³⁰C. Leforestier, F. Gatti, R. S. Fellers, and R. J. Saykally, *J. Chem. Phys.* **117**, 8710 (2002).

³¹C. J. Burnham and S. S. Xantheas, *J. Chem. Phys.* **116**, 1479 (2002).

³²R. Bukowski, K. Szalewicz, G. C. Groenenboom, and A. van der Avoird, *Science* **315**, 1249 (2007); Ad v. d. Avoird and K. Szalewicz, *J. Chem. Phys.* **128**, 014302 (2008); R. Bukowski, K. Szalewicz, G. C. Groenenboom, and A. van der Avoird, *ibid.* **128**, 094313 (2008); **128**, 094314 (2008).

³³X. Huang, B. J. Braams, and J. M. Bowman, *J. Phys. Chem. A* **110**, 445 (2006); X. Huang, B. J. Braams, J. M. Bowman, R. E. A. Kelly, J. Tennyson, G. C. Groenenboom, and A. van der Avoird, *J. Chem. Phys.* **128**, 034312 (2008).

³⁴J. Rodriguez, D. Laria, E. J. Marceca, and D. A. Estrin, *J. Chem. Phys.* **110**, 9039 (1999).

³⁵P. L. Silvestrelli, M. Bernasconi, and M. Parrinello, *Chem. Phys. Lett.* **277**, 478 (1997).

³⁶I. Morrison and S. Jenkins, *Physica B* **263–264**, 442 (1999).

³⁷<http://www.quantum-espresso.org>.

³⁸S. S. Xantheas, *J. Chem. Phys.* **102**, 4505 (1994).

³⁹R. Car and M. Parrinello, *Phys. Rev. Lett.* **55**, 2471 (1985).

⁴⁰P. Tangney and S. Scandolo, *J. Chem. Phys.* **116**, 14 (2002).

⁴¹S. Nosé, *Mol. Phys.* **52**, 255 (1984).

⁴²B. Guillot, *J. Chem. Phys.* **95**, 1543 (1991).

⁴³R. Ramírez, T. López-Ciudad, P. Kumar, and D. Marx, *J. Chem. Phys.* **121**, 3973 (2004).

⁴⁴B. Guillot and Y. Guissani, *J. Chem. Phys.* **108**, 10162 (1998).

⁴⁵M. J. Smit, G. C. Groenenboom, P. E. S. Wormer, A. van der Avoird, R. Bukowski, and K. Szalewicz, *J. Phys. Chem. A* **105**, 6212 (2001).

⁴⁶F. N. Keutsch and R. J. Saykally, *Proc. Natl. Acad. Sci. U.S.A.* **98**, 10533 (2001).

⁴⁷J. Kim and K. S. Kim, *J. Chem. Phys.* **109**, 5886 (1998).

⁴⁸K. S. Kim, M. Dupuis, G. C. Lie, and C. Clementi, *Chem. Phys. Lett.* **131**, 451 (1986).

⁴⁹M. Losada and S. Leutwyler, *J. Chem. Phys.* **117**, 2003 (2002).